Phytochemistry Letters 29 (2019) 41–46

Contents lists available at ScienceDirect

Phytochemistry Letters

journal homepage: www.elsevier.com/locate/phytol

Cytotoxic polyketides from endophytic fungus *Phoma bellidis* harbored in *Ttricyrtis maculate*

Wen-Xuan Wang[1], Mei-Jia Zheng[1], Jing Li, Tao Feng, Zheng-Hui Li, Rong Huang, Yong-Sheng Zheng, Huan Sun, Hong-Lian Ai*, Ji-Kai Liu*

School of Pharmaceutical Sciences, South-Central University for Nationalities, Wuhan, Hubei, 430074, PR China

ARTICLE INFO

Keywords:
Phoma bellidis
Endophytic fungus
Decanolides
Cytotoxicity

ABSTRACT

Four new polyketides, namely bellidisins A-D (**1**-**4**), were isolated from rice fermentation extract of endophytic fungus *Phoma bellidis*, along with three known compounds pinolidoxin (**5**), 5,6-epoxypinolidoxin (**6**), and 2-epi-herbarumin II (**7**). Their structures and absolute configurations were determined by 1D and 2D NMR, HRESIMS and ECD calculation. Their cytotoxicity was evaluated against human cancer cell lines HL-60, A549, SMMC-7721, MCF-7, and SW480. Compound **4** showed significant cytotoxicity on these five cell lines with IC_{50} value ranged from 3.40 to 15.25 μM, which is stronger than cisplatin (4.86–27.70 μM).

1. Introduction

Phoma species are known as widely distributed pathogens, endophytes or soil fungi (Rai et al., 2014; Orlandelli et al., 2015). They can produce diverse secondary metabolites including polyketides, cyclic lipodepsipeptides, alkaloids, and fatty acids, with cytotoxic, neuraminidase inhibitory, squalene synthase inhibitory, antimicrobial, phytotoxic, or HIV-1 reverse transcriptase inhibitory activities (Arora et al., 2016; Bi et al., 2016; Graupner et al., 2003; Herath et al., 2009; Ondeyka et al., 2006; Tan et al., 2018; Zhang et al., 2012).

As the continuum of the research on diverse bioactive compounds from endophytic fungi harbored in medicinal plants (Li and Lou, 2018; Wang et al., 2016), *P. bellidis* was isolated from the healthy leave tissue of medicinal plant *Tricyrtis maculata* which is used for the treatment of blood stasis, asthma, and mental stress (Yan et al., 2017). From the ethyl acetate extract of the rice fermentation of *P. bellidis*, one novel decanolide-derivated polyketide (**1**), and three new decanolides (**2**-**4**) were identified by extensive spectroscopic characterization methods, along with three known compounds, namely pinolidoxin (**5**) (Evidente et al., 1993), 5,6-epoxypinolidoxin (**6**) (Evidente et al., 1993), and 2-epi-herbarumin II (**7**) (Cimmino et al., 2012) (Fig. 1). Diverse bioactivities of this type of decanolides were reported previously, including phytotoxic, antibacterial, and antitumoral activities (García-Fortanet et al., 2005; Sun et al., 2012). In order to discover promising anticancer agents, the cytotoxicity of these isolated compounds was evaluated against five human cancer cell lines.

2. Results and discussion

The molecular formula of compound **1** was determined as $C_{19}H_{28}O_7$ by HRESIMS at *m/z* 367.1761 [M-H]- (calcd for $C_{19}H_{27}O_7$, 367.1762), indicating six degrees of unsaturation. The ^{1}H NMR spectrum of **1** showed the typical signals of a sorbyl group at δ_H 5.82 (1H, d, 15.4, H-14), 7.27 (1H, dd, 15.4, 9.8, H-15), 6.23 (1H, dd, 15.3, 9.8, H-16), 6.20 (1H, dq, 15.3, 5.2, H-17) and 1.89 (3H, dd, 5.2, H-18), one methoxyl group at δ_H 3.49 (3H, s), and one triple methyl peak at δ_H 0.87 (3H, t, 7.3, H-12) (Table 1). The ^{13}C NMR spectrum of **1** associated with HSQC and DEPT experiments indicated one methyl, one methoxyl, four methenes, five methines, one carbonyl, and one aliphatic quaternary carbon, beside the signals of the sorbyl group (Table 2). In ^{1}H-^{1}H COSY experiment, three proton spin-spin systems were confirmed, as depicted in Fig. 2. The HMBC experiment showed correlations between H-6/C-7, H-8/C-7, H-2/C-1, H-3/C-1, H-6/C-1, and 1-OH/C-3 (Fig. 2). According to the mentioned information, the planar structure can be determined as showed in Fig. 2. To deduce the relative configuration of **1**, the ROESY experiment was performed with nuclear Overhauser effects (NOE) observed between H-2/1-OH, 1-OH/H-9, H-6/H-8, and H-8/H-10. Furthermore, the coupling constant between H-6 and H-5 is 10.5 Hz, indicating they are both axial bonds. Therefore, the relative configuration was determined as showed in Fig. 1. ECD calculation of **1** was performed on B3PW91-D3/6-31 G(d) level of theory to identify the absolute configuration. The calculated ECD curve of the 1*R*,2*S*,5*R*,6*R*,8*R*,9*R* enantiomer showed similar tendency to the

* Corresponding authors.
E-mail addresses: aihonglian05@163.com (H.-L. Ai), jkliu@mail.kib.ac.cn (J.-K. Liu).
[1] These authors contributed equally to this work and should be regarded as co-first authors.

https://doi.org/10.1016/j.phytol.2018.11.012
Received 5 August 2018; Received in revised form 13 October 2018; Accepted 8 November 2018
Available online 16 November 2018

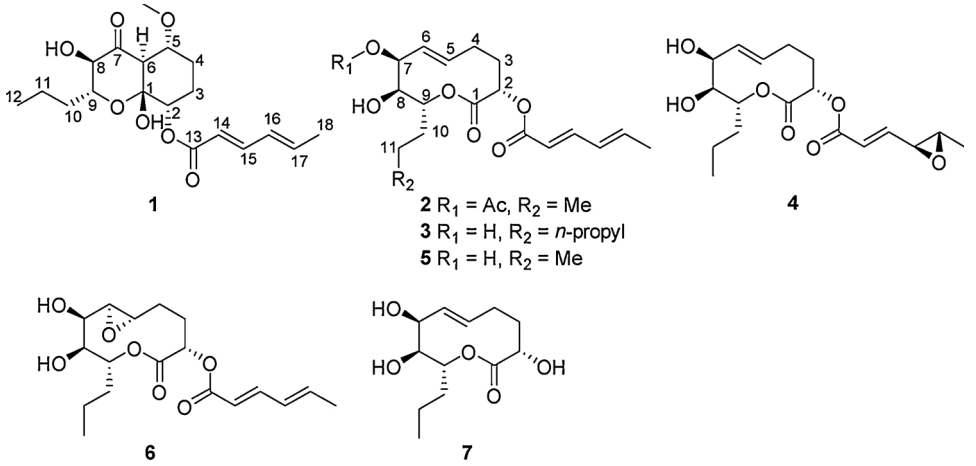

Fig. 1. Structures of compounds **1-7**.

Table 1
^{1}H NMR data of compounds **1-4** ($CDCl_3$, 600 MHz, *J* in Hz).

No.	1	2	3	4
2	5.02 t (2.5)	5.24 dd (5.7, 1.9)	5.26 br d (5.0)	5.21 dd (5.5, 2.0)
3	1.88 overlapped	2.16 overlapped	2.18 m	2.14 ddd (14.0, 3.8, 2.0)
		1.99 m	1.99 m	1.96 ddd (14.0, 5.5, 3.2)
4	2.08 m	2.40 ddd (24.8, 13.1, 4.2)	2.42 br dd (24.0, 13.0)	2.36 m
	1.49 m	2.18 overlapped	2.24 m	2.20 m
5	3.72 ddd (10.5, 10.5, 4.9)	5.35 ddd (15.5, 4.2, 2.3)	5.52 br dd (15.7, 13.0)	5.49 m
6	2.99 d (10.5)	5.60 dd (15.5, 2.3)	5.65 br d (15.7)	5.61 dd (15.9, 1.1)
7		5.56 dd (2.3, 2.3)	4.43 br s	4.42 dd (2.1, 1.1)
8	3.91 d (9.0)	3.70 dd (9.6, 2.3)	3.52 br d (10.0)	3.49 dd (9.6, 2.1)
9	3.76 ddd (9.0, 8.5, 2.4)	5.18 dd (9.6, 9.6, 2.5)	5.00 br dd (10.0, 10.0)	5.03 ddd (9.6, 9.6, 2.6)
10	1.79 m	1.47 m	1.52 m	1.76 m
	1.62 m	1.73 m	1.80 m	1.47 m
11	1.45 m	1.23 m	1.27 overlapped	1.29 m
	1.29 m	1.32 m		1.17 m
12	0.87 t (7.3)	0.88 t (7.4)	1.26 overlapped	0.84 t (7.4)
13			1.26 overlapped	
14	5.82 d (15.4)	5.86 d (15.4)	0.85 t (6.3)	6.20 d (15.3)
15	7.27 dd (15.4, 9.8)	7.31 dd (10.0, 15.4)		6.74 dd (15.3, 6.6)
16	6.23 dd (15.3, 9.8)	6.25 m	5.87 d (15.4)	3.22 dd (6.6, 2.0)
17	6.20 dq (15.3, 5.2)	6.20 m	7.31 dd (15.4, 10.0)	3.00 td (5.1, 2.0)
18	1.89 d (5.2, 3 H)	1.89 d (5.8)	6.25 m	1.40 d (5.1)
19			6.20 m	
20			1.89 d (6.0)	
5-OMe	3.49 s			
1-OH	3.22 s			
8-OH	3.60 s			
AcO-7	–	2.20 s		

experimental ECD data (Fig. 3). Therefore, the absolute configuration of **1** was determined.

Compound **2** was obtained as a colorless oil. Its molecular formula was determined as $C_{20}H_{28}O_7$ by HRESIMS at *m/z* 425.1817 $[M + HCOO]^-$ (calcd for $C_{21}H_{29}O_9$, 425.1817), suggesting seven degrees of unsaturation. The ^{1}H NMR and ^{13}C NMR spectra of **2** showed very similar signals to **5** (molecular formula $C_{18}H_{26}O_6$), except extra signals of acetyl (δ_H 2.20, δ_C 171.5, 21.2), suggesting **2** is a acetylated derivative of **5**. Further ^{1}H-^{1}H COSY and HMBC experiments confirmed the planar structure of the core moiety of **2** is the same as **5** (Fig. 4). In the HMBC experiment, the correlation between H-7 and acetyl group (δ_C 171.5) was observed, which suggested that the acetyl group connects to the oxygen at position 7 as showed in Fig. 4. The coupling constants of H-2, H-8, and H-9 indicated that they are equatorial, equatorial, and axial bonds respectively (Table 1), which can also be confirmed by ROESY experiment (Fig. 4).

Compound **3** was a colorless oil. Its molecular formula was determined as $C_{20}H_{30}O_6$ by HRESIMS at *m/z* 411.2022 $[M + HCOO]^-$ (calcd for $C_{21}H_{31}O_8$, 411.2024), indicating six degrees of unsaturation. Comparing to the formula of **5**, **3** has two more carbons and four more hydrogens. The ^{1}H NMR spectrum of **3** (Table 1) showed similar signals to **5**, including the signals of the sorbyl group and the decanolide core structure (Table 1). The ^{13}C NMR (Table 2) and DEPT spectra of **3** showed two more methene groups (δ_C 31.5, 22.5) than **5**, which is consistent with the determined formula. The ^{1}H-^{1}H COSY experiment showed a spin-spin system from H-2 to H-14. Moreover, the HMBC correlations between H-9 and C-1 as well as H-2 and C-15 suggested the planar structure of the core moiety and the connection of sorbyl group are the same as **5**. The difference between them is the substituent group of **3** at position 9 is *n*-pentyl group. The chemical shifts and coupling

Table 2
^{13}C NMR data of compounds **1**-**4** ($CDCl_3$, 150 MHz).

No.	1	2	3	4
1	100.4	171.0	172.0	171.5
2	71.5	70.0	69.7	70.2
3	24.7	29.6	29.9	29.8
4	24.5	27.6	27.4	27.4
5	73.7	123.4	123.0	122.7
6	56.8	128.7	132.3	132.7
7	205.7	74.9	73.1	73.0
8	76.8	72.3	73.1	73.1
9	77.8	71.9	71.5	71.5
10	34.9	33.7	31.4	33.7
11	18.2	17.4	23.7	17.5
12	14.1	14.1	31.5	14.0
13	166.5	166.2	22.5	164.6
14	118.5	118.2	14.0	122.9
15	146.2	146.0	166.1	145.8
16	129.8	129.8	118.1	57.3
17	140.6	140.5	146.0	57.9
18	18.9	18.9	129.7	17.6
19			140.3	
20			18.8	
5-OMe	57.7			
CO(AcO-7)		171.5		
CH_3(AcO-7)		21.2		

constants of H-2, H-7 and H-8 as well as the ROESY experiment confirmed the relative configuration of **3** is the same as **5** (Fig. 5).

Compound **4** was a colorless oil. Its molecular formula was determined to be $C_{18}H_{26}O_7$ by HRESIMS at *m/z* 399.1657 $[M + HCOO]^-$ (calcd for $C_{19}H_{27}O_9$, 399.1660), indicating six degrees of unsaturation. The ^1H NMR (Table 1) and ^{13}C NMR (Table 2) spectra of **4** showed the signals of the core structure were similar to the data of **5**. However, it has different signals of the substituent group at position 2, namely δ_H 6.20 (1H, d, 15.3, H-14), 6.74 (1H, dd, 15.3, 6.6, H-15), 3.22 (1H, dd, 6.6, 2.0, H-16), 3.00 (1H, dd, 5.1, 2.0, H-17), 1.40 (3H, d, 5.1, Me-18), and δ_C 164.6, 122.9, 145.8, 57.3, 57.9, 17.6. Comparing to the reported ^1H NMR and ^{13}C NMR data of 4,5-epoxyhexenoic acid (Ueki and Kinoshita, 2004), this moiety was deduced to be 4,5-epoxyhexenoyl group, which was also confirmed by HMBC correlations and ^1H-^1H COSY experiment (Fig. 6). In the ROESY experiment, NOEs were observed between H-15/H-17 and H-16/Me-18, indicating the relative configuration of the epoxy group is as showed in Fig. 6. Because the stereo distance between the chiral center of 16,17-epoxy and the core structure far beyond the maximum distance for NOE, it is not possible to deduce the configuration of 16,17-epoxy group related to the core structure by ROESY experiment. Fortunately, excited states analysis on B3PW91-D3/6–31 G(d) level of theory showed that the n- > π^* excitation of the oxygen in the 16,17-epoxy group is involved in the main Cotton effect of the ECD spectrum at 232 nm (Fig. S46, Table S1). Therefore, the difference between the ECD curves of two possible configurations (2*S*,7*S*,8*S*,9*R*,16*S*,17*S* and 2*S*,7*S*,8*S*,9*R*,16*R*,17*R*) may be sufficient to distinguish these two epimers. As showed in Fig. 7, the calculated ECD curve of 2*S*,7*S*,8*S*,9*R*,16*S*,17*S* epimer matches the experimental data very well, while the ECD curve of 2*S*,7*S*,8*S*,9*R*,16*R*,17*R* epimer is different from it. Therefore, the absolute configuration of **4** was determined to be 2*S*,7*S*,8*S*,9*R*,16*S*,17*S*.

Compounds **5**-**7** are known, but the configuration of the 5,6-epoxy group in compound **6** was not assigned in the previous report (Evidente et al., 1993). Herein, we determined it to be 5*S*,6*S*-epoxy by ROESY experiment as showed in Fig. S41.

Different from compounds **2**-**5**, **1** has a carbon skeleton having a fused pyran and cyclohexane ring system, which is supposed to be formed by Claisen condensation from **5**. The biosynthesis pathway of **1** is proposed in Fig. 8.

In previous investigation, microcarpalide, a decanolide type compound, was reported as a strong microfilament disrupting agent (Ratnayake et al., 2001). In order to unveil the anticancer potential of these compounds, therefore, we performed cytotoxicity assay against five human cell lines for compounds **1**-**7** (Table 3). Compound **4** showed significant cytotoxicity against these cell lines especially against human leukemia cell line HL-60 (IC_{50} value 3.40 ± 0.11 μM). Markedly, the performance of **4** was better than the clinical drug cisplatin. Comparing to the structures of nonactive compounds **2**, **3**, **5**-**7**, the 4*S*,5*S*-4,5-epoxyhexenoyl group in **4** is probably the key pharmacophore for its cytotoxicity. Moreover, compound **1** only showed moderate cytotoxicity against HL-60 cell lines. The other compounds didn't show cytotoxicity in this assay (IC_{50} > 40 μM).

3. Experimental

3.1. General experimental procedures

Optical rotations were measured with a Jasco model 1020 polarimeter (Horiba, Tokyo, Japan). UV spectra were measured on a UV-2450 spectrometer (SHIMADZU, Kyoto, Japan). CD spectra were recorded with an Applied Photophysics spectrometer (Chirascan, New Haven, USA). HRESIMS spectra were measured on Q Exactive Obitrap mass spectrometer (ThermoFisher Scientific, USA). NMR spectra were recorded on a Bruker AV-600 spectrometer (Bruker, Karlsruhe, Germany) with TMS as an internal standard. Macroporous resin D101 (Cang Zhou Bon Adsorber Technology Co. Ltd., Hebei, China), and silica gel (Qingdao Marine Chemical Factory, Qingdao, China) were used for column chromatography (CC). Thin layer chromatography (TLC) experiments were performed on silica gel GF-254 pre-coated on glass plates (Qingdao Marine Chemical Factory, Qingdao, China). Semi-preparative-HPLC experiments were carried on Agilent 1260 HPLC with Agilent Zorbax SB-C18 column (5 μm, 150 × 9.4 mm). All solvents were analytical grade.

3.2. Culture and fermentation of Fungal material

The strain *P. bellidis* was isolated from the healthy leave tissue of *Tricyrtis maculata* following the reported standard surface sterilization and culture procedure (Wang et al., 2015). The fungal strain was cultivated on potato dextrose agar at 25 °C for 7 days for identification. The internal transcribed spacer (ITS) sequencing was performed with the established methods (Wang et al., 2015). The resulted ITS sequence of this strain is almost identical with the strain deposited at Genbank with accession number KM507775.1 (max identity: 99%, query cover: 99%). The fungus was deposited in the internal culture bank at School of Pharmaceutical Sciences, South-Central University for Nationalities, Hubei, China, with designation number HGX2.

Large scale fermentation of *P. bellidis* was performed on 5 kg solid rice medium (50 g rice, 50 mL water, in each 250 mL Erlenmeyer flask) at 25 °C for 30 days.

3.3. Extraction and isolation

The fermented rice medium was collected and extracted with 10 L ethyl acetate for 3 times. Solvent was removed by rotary evaporator to yield 95 g dark brown crude extract. The extract was absorbed on 500 g macroporous resin D101, and then successively eluted by water, 80% aquatic MeOH, and 100% MeOH. The 80% aquatic MeOH portion was collected and condensed to yield 74 g residue.

The 80% MeOH portion was subjected to silica gel column and

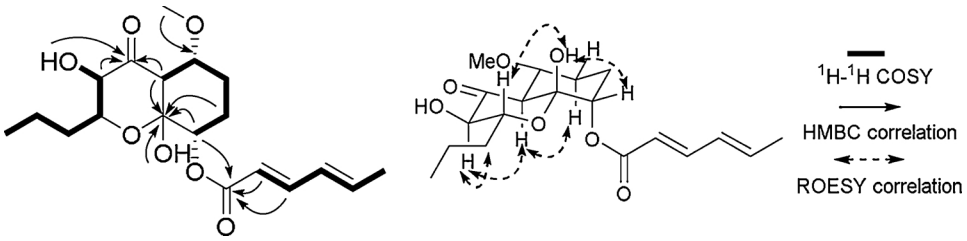

Fig. 2. Key 2D NMR correlations of **1**.

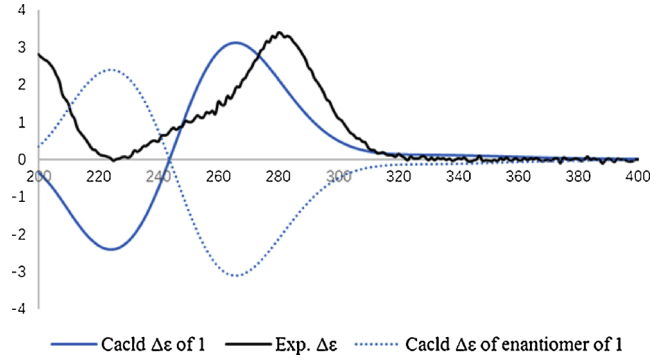

Fig. 3. Calculated ECD curve of **1** (blue solid), calculated ECD curve of the enantiomer of **1** (blue dashed), and experimental ECD data of **1** (black) (For interpretation of the references to colour in this figure legend, the reader is referred to the web version of this article).

eluted with petroleum ether and ethyl acetate (gradient 1:0 ~ 0:1) to yield 5 fractions (Fr.A-Fr.E). The Fr.A was subjected on silica gel column and eluted with $CHCl_3$ with two sub-fractions obtained (Fr.A1 and Fr.A2). The Fr.A1 sub-fraction was purified on semi-preparative HPLC to yield compounds **1**-**3** and **5** (10.3 mg, 9.1 mg, 10.3 mg, and 100.1 mg respectively) with gradient mobile phase (45%–55% acetonitrile, 20 min, 4 mL/min). The retention time (t_R) of them was 6.5 min, 11.5 min, 13.5 min and 7.6 min respectively. From Fr.B, compound **5** (8.3 g) was purified with silica gel column with petroleum ether and ethyl acetate (5:1). Fr.C was subjected on silica gel column and eluted with $CHCl_3$ and ethyl acetate (gradient 10:1 ~ 0:1), to yield two sub-fractions (Fr.C1 and Fr.C2). The Fr.C2 was successively purified by semi-preparative HPLC to yield compounds **4** (50.5 mg, 35% acetonitrile, 4 mL/min, t_R 9.6 min), and **6** (34.0 mg, 60% MeOH, 3 mL/min, t_R 6.9 min). The Fr.D was recrystallized in $CHCl_3$ and MeOH (1:1) to yield compound **7** (100.2 mg).

3.3.1. Bellidisin A (1)

Colorless oil; [α]25 D +55.26 (*c* 0.04, MeOH); IR(KBr): υ_{max} 1655.5, 3487.3 cm^{-1}; HPLC-UV (in ACN-H_2O) λ_{max} 265 nm; CD (MeOH) 200 (Δε +2.81), 225 (Δε -0.02), 280 (Δε +3.40) nm; ^{1}H NMR (600 MHz in $CDCl_3$) and ^{13}C NMR (150 MHz in $CDCl_3$) data, see Tables 1 and 2; HRESIMS *m/z* 367.1761 [M-H]- (calcd for $C_{19}H_{27}O_7$, 367.1762).

3.3.2. Bellidisin B (2)

Colorless oil; [α]25 D +128.95 (*c* 0.04, MeOH); IR(KBr): υ_{max} 1653.0, 1718.6, 3500.8 cm^{-1}; HPLC-UV (in ACN-H_2O) λ_{max} 265 nm; CD (MeOH) 200 (Δε +2.84), 217 (Δε -6.41), 254 (Δε +12.26) nm; ^{1}H NMR (600 MHz in $CDCl_3$) and ^{13}C NMR (150 MHz in $CDCl_3$) data, see Tables 1 and 2; HRESIMS *m/z* 425.1817 [M + HCOO]- (calcd for $C_{21}H_{29}O_9$, 425.1817).

3.3.3. Bellidisin C (3)

Colorless oil; [α]25 D +138.14 (*c* 0.04, MeOH); IR(KBr): υ_{max} 1645.3, 1716.7, 3319 cm^{-1}; HPLC-UV (in ACN-H_2O) λ_{max} 264 nm; CD (MeOH) 200 (Δε +1.80), 216 (Δε -5.87), 256 (Δε +15.42) nm; ^{1}H NMR (600 MHz in $CDCl_3$) and ^{13}C NMR (150 MHz in $CDCl_3$) data, see Tables 1 and 2; HRESIMS *m/z* 411.2022 [M + HCOO]- (calcd for $C_{21}H_{31}O_8$, 411.2024).

3.3.4. Bellidisin D (4)

Colorless oil; [α]25 D +748.9 (*c* 0.03, MeOH); IR(KBr): υ_{max} 1724.4, 3552.9 cm^{-1}; HPLC-UV (in ACN-H_2O) λ_{max} 220 nm; CD (MeOH) 224 (Δε +19.64), 258 (Δε -0.40) nm; ^{1}H NMR (600 MHz in $CDCl_3$) and ^{13}C NMR (150 MHz in $CDCl_3$) data, see Tables 1 and 2; HRESIMS *m/z* 399.1657 [M + HCOO]- (calcd for $C_{19}H_{27}O_9$, 399.1660).

3.4. ECD calculation

Confab was used to search the local low-energy conformers of compounds **1**, **4**, and their enantiomer or epimers (O'Boyle et al., 2011). The generated conformers were further optimized by semi-empirical method PM7 (Stewart, 2013) with MOPAC2016 (Stewart, 2016), and the conformers with Boltzmann population more than 1% were subjected to further optimization, frequency and ECD calculations (TDDFT) on B3PW91-D3/6–31 G(d) level of theory with IEFPCM solvation model (MeOH) by Gaussian09 (Frisch et al., 2016). The calculated ECD data of all conformers were Boltzmann averaged by Gibbs free energy, and compared with experimental data of compounds **1** and **4**.

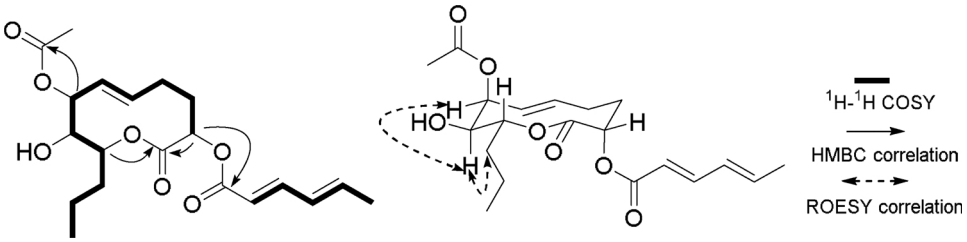

Fig. 4. Key 2D NMR correlations of **2**.

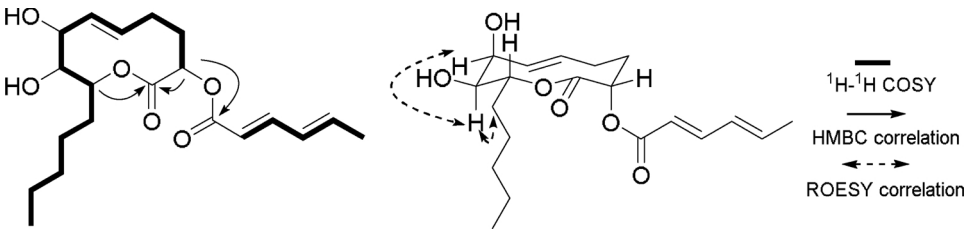

Fig. 5. Key 2D NMR correlations of **3**.

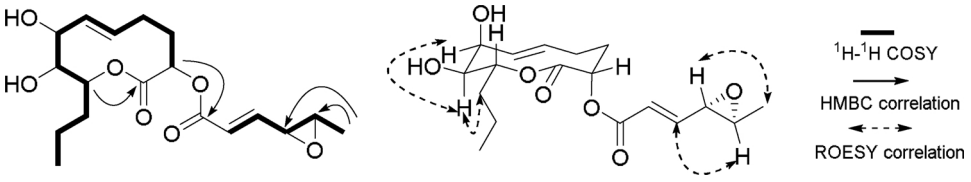

Fig. 6. Key 2D NMR correlations of **4**.

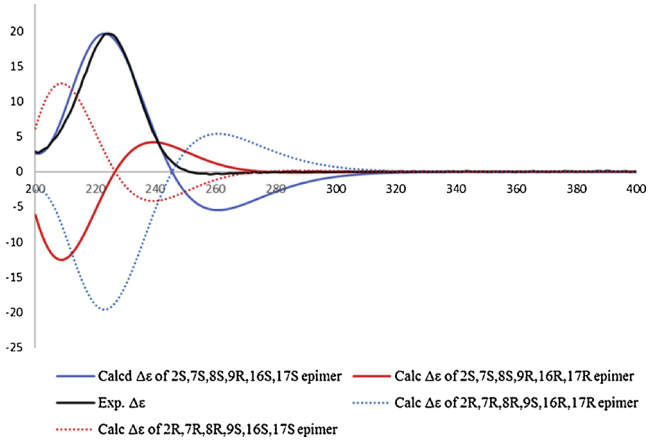

Fig. 7. Calculated ECD curve of the 2*S*,7*S*,8*S*,9*R*,16*S*,17*S* epimer (blue), calculated ECD curve of the 2*S*,7*S*,8*S*,9*R*,16*R*,17*R* epimer (red), and experimental ECD data of **4** (black). All the calculated curves were blue shifted with 10 nm (For interpretation of the references to colour in this figure legend, the reader is referred to the web version of this article).

3.5. MTS cytotoxicity assay

The human leukaemia cell line HL-60, adenocarcinomic human alveolar basal epithelial cells A549, human breast cancer cell line MCF-7, and human colorectal adenocarcinoma cell line SW480 were purchased from American Type Culture Collection (ATCC, Manassas, VA, USA), while human hepatocarcinoma cell line SMMC-7721 was bought from China Infrastructure of Cell Line Resources (Beijing, China). All cell lines were cultured in DMEM medium, with the supplementation of 10% fetal bovine serum (FBS), 100 units/mL penicillin, and 100 units/mL streptomycin (Invitrogen, Carlsbad, CA, USA) at 37 °C in humidified environment with 5% CO_2. Each tested compounds were prepared into gradient concentration namely 40 μM, 8 μM, 1.6 μM, 0.32 μM, and 0.064 μM in DMSO. Cisplatin (Sigma-Aldrich, 99%) was used as a positive control for comparison. The cell lines were treated with compounds for 48 h in triplicates. The cytotoxicity assay was performed with MTS method, following the reported procedure (Huang et al., 2017).

4. Conclusion

Herein, we reported seven polyketides (**1**-**7**) from the rice ferments of endophytic fungus *P. bellidis*. The structures of the new compounds **1**-**4** were deduced by spectroscopic analysis, and the absolute configurations of **2** and **4** were determined by ECD calculation, including the configuration of the epoxy group on the flexible side chain of **4**. In the cytotoxicity assay, compound **4** showed marked activities against tested cell lines, and its mode of action will be investigated in the following project.

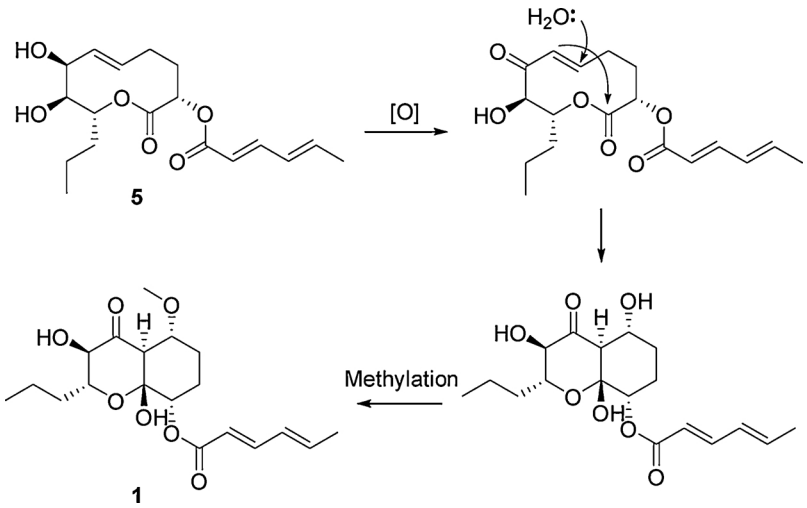

Fig. 8. The proposed biosynthesis pathway from **5** to **1**.

Table 3
Cytotoxicity of compounds **1** and **4** against five human cancer cell lines (IC_{50} in μM ± SD).

Compound	HL-60	A-549	SMMC-7721	MCF-7	SW480
1	20.62 ± 0.46	> 40	> 40	> 40	> 40
4	3.40 ± 0.26	14.80 ± 0.44	11.39 ± 1.18	15.25 ± 0.07	8.55 ± 0.21
Cisplatin	4.86 ± 0.11	25.61 ± 0.64	21.13 ± 1.22	23.59 ± 1.34	27.70 ± 1.59

Conflict of interest

The authors declare no conflict of interest.

Acknowledgements

This research was financially supported by National Natural Science Foundation of China [No. 31560010, 81773590, 81561148013, 21502239], National Key R&D Plan [No. 2017YFC1704007], Hubei Provincial Natural Science Foundation of China [No. 2018CFB222], Key Projects of Technological Innovation of Hubei Province [No. 2016ACA138], and the Fundamental Research Funds for the Central Universities, South-Central University for Nationalities [No. CZP18005, CZT18013, CZT18014]. We are grateful for the convenience for the HRMS and NMR measurement provided by Analytical & Measuring Center, School of Pharmaceutical Sciences, South-Central University for Nationalities. We thank Kunming Institute of Botany, Chinese Academy of Sciences for doing the quantum chemistry calculation on high performance computing cluster.

Appendix A. Supplementary data

Supplementary material related to this article can be found, in the online version, at doi:https://doi.org/10.1016/j.phytol.2018.11.012.

References

Arora, P., Wani, Z.A., Nalli, Y., Ali, A., Riyaz-Ul-Hassan, S., 2016. Antimicrobial potential of thiodiketopiperazine derivatives produced by *Phoma* sp., an endophyte of *Glycyrrhiza glabra* Linn. Microb. Ecol. 72, 802–812.

Bi, R., Lawoko, M., Henriksson, G., 2016. *Phoma herbarum*, a soil fungus able to grow on natural lignin and synthetic lignin (DHP) as sole carbon source and cause lignin degradation. J. Ind. Microbiol. Biotechnol. 43, 1175–1182.

Cimmino, A., Andolfi, A., Fondevilla, S., Abouzeid, M.A., Rubiales, D., Evidente, A., 2012. Pinolide, a new nonenolide produced by *Didymella pinodes*, the causal agent of ascochyta blight on *Pisum sativum*. J. Agric. Food Chem. 60, 5273–5278.

Evidente, A., Capasso, R., Abouzeid, M.A., 1993. Three new toxic pinolidoxins from Ascochyta pinodes. J. Nat. Prod. 56, 1937–1943.

Frisch M.J., Trucks G.W., Schlegel H.B., Scuseria G.E., Robb M.A., Cheeseman J.R., Scalmani G., Barone V., Petersson G.A., Nakatsuji H., Li X., Caricato M., Marenich A., Bloino J., Janesko B.G., Gomperts R., Mennucci B., Hratchian H.P., Ortiz J.V., Izmaylov A.F., Sonnenberg J.L., Williams-Young D., Ding F., Lipparini F., Egidi F., Goings J., Peng B., Petrone A., Henderson T., Ranasinghe D., Zakrzewski V.G., Gao J., Rega N., Zheng G., Liang W., Hada M., Ehara M., Toyota K., Fukuda R., Hasegawa J., Ishida M., Nakajima T., Honda Y., Kitao O., Nakai H., Vreven T., Throssell K., Montgomery Jr. J.A., Peralta J.E., Ogliaro F., Bearpark M., Heyd J.J., Brothers E., Kudin K.N., Staroverov V.N., Keith T., Kobayashi R., Normand J., Raghavachari K., Rendell A., Burant J.C., Iyengar S.S., Tomasi J., Cossi M., Millam J.M., Klene M., Adamo C., Cammi R., Ochterski J.W., Martin R.L., Morokuma K., Farkas O., Foresman J.B., Fox D.J., 2016. Gaussian, Inc., Wallingford CT.

García-Fortanet, J., Murga, J., Falomir, E., Carda, M., Marco, J.A., 2005. Stereoselective total synthesis and absolute configuration of the natural decanolides (-)-microcarpalide and (+)-lethaloxin. Identity of (+)-lethaloxin and (+)-pinolidoxin. J. Org. Chem. 70, 9822–9827.

Graupner, P.R., Carr, A., Clancy, E., Gilbert, J., Bailey, K.L., Derby, J.A., Gerwick, B.C., 2003. The macrocidins: novel cyclic tetramic acids with herbicidal activity produced by Phoma macrostoma. J. Nat. Prod. 66, 1558–1561.

Herath, K., Harris, G., Jayasuriya, H., Zink, D., Smith, S., Vicente, F., Bills, G., Collado, J., González, A., Jiang, B., Kahn, J.N., Galuska, S., Giacobbe, R., Abruzzo, G., Hickey, E., Liberator, P., Xu, D., Roemer, T., Singh, S.B., 2009. Isolation, structure and biological activity of phomafungin, a cyclic lipodepsipeptide from a widespread tropical *Phoma* sp. Bioorg. Med. Chem. 17, 1361–1369.

Huang, Y., Zhang, S.B., Chen, H.P., Zhao, Z.Z., Zhou, Z.Y., Li, Z.H., Feng, T., Liu, J.K., 2017. New Acetylenic Acids and derivatives from the edible mushroom *Craterellus lutescens* (Cantharellaceae). J. Agric. Food Chem. 65, 3835–3841.

Li, G., Lou, H.X., 2018. Strategies to diversify natural products for drug discovery. Med. Res. Rev. 38, 1255–1294.

O'Boyle, N.M., Vandermeersch, T., Flynn, C.J., Maguire, A.R., Hutchison, G.R., 2011. Confab - Systematic generation of diverse low-energy conformers. J. Cheminform. 3, 8.

Ondeyka, J.G., Zink, D.L., Young, K., Painter, R., Kodali, S., Galgoci, A., Collado, J., Tormo, J.R., Basilio, A., Vicente, F., Wang, J., Singh, S.B., 2006. Discovery of bacterial fatty acid synthase inhibitors from a *Phoma* species as antimicrobial agents using a new antisense-based strategy. J. Nat. Prod. 69, 377–380.

Orlandelli, R.C., de Almeida, T.T., Alberto, R.N., Polonio, J.C., Azevedo, J.L., Pamphile, J.A., 2015. Antifungal and proteolytic activities of endophytic fungi isolated from *Piper hispidum* Sw. Braz. J. Microbiol. 46, 359–366.

Rai, M.K., Tiwari, V.V., Irinyi, L., Kövics, G.J., 2014. Advances in taxonomy of genus *Phoma*: polyphyletic nature and role of phenotypic traits and molecular systematics. Indian J. Microbiol. 54, 123–128.

Ratnayake, A.S., Yoshida, W.Y., Mooberry, S.L., Hemscheidt, T., 2001. The structure of microcarpalide, a microfilament disrupting agent from an endophytic fungus. Org. Lett. 3, 3479–3481.

Stewart, J.J.P., 2013. Optimization of parameters for semiempirical methods VI: more modifications to the NDDO approximations and re-optimization of parameters. J. Mol. Model. 19, 1–32.

Stewart, J.J.P., 2016. Stewart Computational Chemistry. Colorado Springs, CO, USA. HTTP://OpenMOPAC.net.

Sun, P., Lu, S., Ree, T.V., Krohn, K., Li, L., Zhang, W., 2012. Nonanolides of natural origin: structure, synthesis, and biological activity. Curr. Med. Chem. 19, 3417–3455.

Tan, X.M., Li, L.Y., Sun, L.Y., Sun, B.D., Niu, S.B., Wang, M.H., Zhang, X.Y., Sun, W.S., Zhang, G.S., Deng, H., Xing, X.K., Zou, Z.M., Ding, G., 2018. Spiciferone analogs from an endophytic fungus *Phoma betae* collected from desert plants in West China. J. Antibiot. (Tokyo) 71, 613–617.

Ueki, T., Kinoshita, T., 2004. Stereoselective synthesis and structure of butalactin and lactone II isolated from *Streptomyces* species. Org. Biomol. Chem. 2, 2777–2785.

Wang, W.X., Kusari, S., Sezgin, S., Lamshöft, M., Kusari, P., Kayser, O., Spiteller, M., 2015. Hexacyclopeptides secreted by an endophytic fungus *Fusarium solani* N06 act as crosstalk molecules in *Narcissus tazetta*. Appl. Microbiol. Biotechnol. 99, 7651–7662.

Wang, W.X., Kusari, S., Laatsch, H., Golz, C., Kusari, P., Strohmann, C., Kayser, O., Spiteller, M., 2016. Antibacterial azaphilones from an endophytic fungus, *Colletotrichum* sp. BS4. J. Nat. Prod. 79, 704–710.

Yan, R., Zhao, H., Wang, X., 2017. Content and accumulation of total flavonoids in *Tricyrtis maculata* Machride, China. Sciencepaper 12, 2109–2113.

Zhang, G.F., Han, W.B., Cui, J.T., Ng, S.W., Guo, Z.K., Tan, R.X., Ge, H.M., 2012. Neuraminidase inhibitory polyketides from the marine-derived fungus Phoma herbarum. Planta Med. 78, 76–78.